Solid State Electronics 159 (2019) 43–50

Contents lists available at ScienceDirect

Solid State Electronics

journal homepage: www.elsevier.com/locate/sse

Current and shot noise at spin-dependent hopping through junctions with ferromagnetic contacts

Viktor Sverdlov[a,b,*], Siegfried Selberherr[b]

[a] Christian Doppler Laboratory for Nonvolatile Magnetoresistive Memory and Logic at the Institute for Microelectronics, TU Wien, Gußhausstraße 27-29, A-1040 Wien, Austria

[b] Institute for Microelectronics, TU Wien, Gußhausstraße 27-29, A-1040 Wien, Austria

ARTICLE INFO

Keywords:
Spin-dependent hopping
Shot noise
Spin relaxation
MTJ
MRAM

ABSTRACT

Upcoming mass production of energy efficient spin-transfer torque magnetoresistive random access memory will revolutionize microelectronics by introducing non-volatility not only in memory but also in logic. The pressing issue is to boost the sensing margin by improving the tunneling magnetoresistance ratio. We demonstrate that spin-dependent trap-assisted tunneling in magnetic tunnel junctions can increase the tunneling magnetoresistance ratio. The impact of spin decoherence and relaxation on the current and shot noise at trap-assisted hopping is investigated in both normal contact-trap-ferromagnet and ferromagnet-trap-ferromagnet systems. In addition, our approach resolves a controversy between the two theoretical approaches to spin-dependent trap-assisted tunneling available in literature.

1. Introduction

Energy efficient spin-transfer torque magnetoresistive random access memory (MRAM) will restructure upcoming microelectronic circuitry by introducing non-volatility not only for memory but also for logic [1]. Boosting the sensing margin by improving the tunneling magnetoresistance ratio (TMR) is an important challenge currently under intense investigation. With reducing dimensions of magnetic tunnel junctions (MTJs) many interesting phenomena due to the correlated spin-charge transport appear.

The Coulomb interaction leads to the repulsion of the charges on a trap. This repulsion leads to the Coulomb blockade, when the double occupancy of the trap is prohibited, which results in strong charge transport correlations. Indeed, when electrons tunnel through the trap [2], a second electron from a metallic contact cannot enter the trap, if it is already occupied by an electron. However, when the electron is released from the trap to a contact, the Coulomb repulsion does not prevent the second electron entering the trap. The electron transport is performed in sequences consisting of an electron hopping from the source electrode to the trap, followed by the electron escaping the trap to the drain electrode. Because the Coulomb repulsion is a purely classical interaction, the electron tunneling through the trap represents an example of classically correlated charge transport.

The Pauli exclusion principle forbidding two electrons with the same spin projections to occupy the trap quantum state results in yet another correlations affecting the transport through the double-quantum dot system in a magnetic field [3]. These spin correlations were recently reported to be responsible for large magnetoresistance and magnetoluminescence effects observed at room temperature in organic semiconductors and organic light-emitting diodes [4].

In case of ferromagnetic contacts, the electron impinging an electrode from a trap has a larger probability to be accommodated by the electrode, if its spin is parallel to the magnetization of the electrode [5]. In this case the drain electrode plays a role similar to the second quantum dot in the Pauli spin blockade experiments [3]. The drain electrode-induced spin correlations result in the Pauli blockade-like trap-assisted tunneling transport between the ferromagnetic electrodes. This spin-dependent resonant tunneling is believed to be responsible for the large magnetoresistance modulation [5] observed in three-terminal spin accumulation experiments [6–10]. Although the role of traps regarding the magnetoresistance is still actively debated [11–13], the non-equilibrium spin injection in silicon as a source of the large signal is reliably ruled out by the latest convincing experiments [14], where two ferromagnetic electrodes in parallel and anti-parallel configurations were employed to inject the spins.

Albeit the spin-dependent tunneling remains the main candidate to explain the large magnetoresistance observed in three-terminal experiments, spin-dependent hopping continues to attract attention, with a different expression for the magnetoresistance dependence on the magnetic filed recently reported [15].

* Corresponding author.
E-mail addresses: Sverdlov@iue.tuwien.ac.at (V. Sverdlov), Selberherr@iue.tuwien.ac.at (S. Selberherr).

https://doi.org/10.1016/j.sse.2019.03.053

Available online 19 March 2019
0038-1101/ © 2019 Elsevier Ltd. All rights reserved.

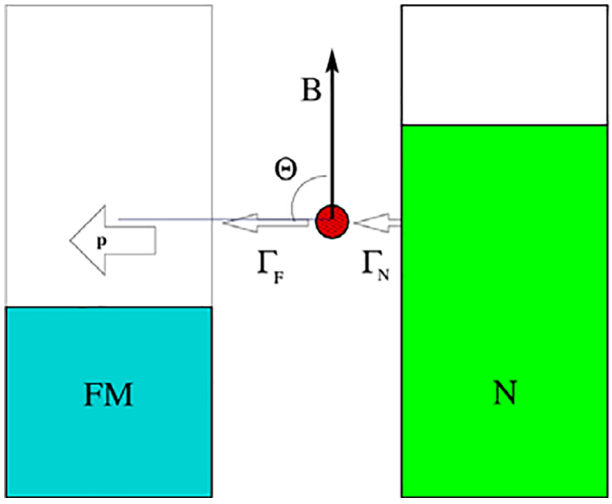

Fig. 1. An electron tunnels with the rate Γ_N on the trap and Γ_F to the ferromagnet. A magnetic field **B** defines the trap spin quantization axis, which is at an angle Θ to the magnetization orientation in the ferromagnetic contact.

To resolve the controversy between the theoretical results [6,15], we generalize the spin-independent hopping in normal metal/oxide/ferromagnet structures to incorporate the electron spin [16]. We first evaluate the stationary current and its low-frequency current fluctuations (shot noise) by a Monte Carlo algorithm [17–19]. We determine that in the general case of spin-dependent hopping the transition rates are determined by a 4 × 4 transition matrix, in contrast to only two rates for spin-up and spin-down considered in [15]. We then investigate the current and the low-frequency current fluctuations described by the spin-dependent trap-assisted hopping in magnetic tunnel junctions based on a ferromagnet/oxide/ferromagnet structure.

2. Method

The master equation for the spin density matrix $\rho_{\sigma\sigma'}$ ($\sigma, \sigma' = \pm$) was recently derived in [6] from the Anderson impurity model in the limit of large on-site interaction. In the basis with the quantization axis chosen along the magnetization direction (Fig. 1) in the ferromagnetic contact the corresponding equations are [6]:

$$\frac{d}{dt}\rho_{\sigma\sigma} = \frac{\Gamma_N}{2}(1-n) - \Gamma_\sigma\rho_{\sigma\sigma} + \omega_L\sin(\Theta)\mathrm{Im}(\rho_{-\sigma\sigma}), \qquad \sigma = \pm \tag{1}$$

$$\frac{d}{dt}\rho_{\sigma-\sigma} = i\omega_L(\sin(\Theta)(\rho_{-\sigma-\sigma} - \rho_{\sigma\sigma})/2 \pm \cos(\Theta)\rho_{\sigma-\sigma}) - \frac{\Gamma_\sigma + \Gamma_{-\sigma}}{2}\rho_{\sigma-\sigma}, \quad -\sigma = \mp \tag{2}$$

Here $0 \le n \le 1$ is the averaged trap occupation. The tunneling rate Γ_N from silicon to a trap does not depend on spin, while the tunneling rate from the trap to a ferromagnet depends on the spin projection $\sigma = \pm$ on the magnetization direction:

$$\Gamma_\pm = \Gamma_F(1 \pm p) \tag{3}$$

The current polarization at the interface of the ferromagnet $p \le 1$ is defined as

$$p = \frac{\Gamma_+ - \Gamma_-}{2\Gamma_F}. \tag{4}$$

The external magnetic field **B** at the impurity position applied in the XZ plane is assumed to form an angle Θ with the magnetization direction in the ferromagnetic lead. The magnetic field **B** enters into the Eqs. (1) and (2) via the spin Larmor precession frequency

$$\omega_L = |\boldsymbol{\omega}_L| = \left|\frac{e\mathbf{B}}{mc}\right|, \tag{5}$$

where e and m are the electron charge and the mass, c is the velocity of light. In (1) Im denotes the imaginary part and in (2) i is the imaginary unit.

The time dependence of the diagonal elements of the density matrix (1) is governed by the balance of the first influx term from the normal electrode on the trap and the second out-flux term to the ferromagnet. The influx term is proportional to the tunneling rate Γ_N multiplied by the probability

$$P_0 = 1 - n, \tag{6}$$

that the site is empty. The one-half coefficient in the first term of (1) is due to the fact that the electron tunneling from the normal electrode can occupy the site with equal probabilities for a spin projection σ up or down.

The second out-flux term is proportional to the probability that the state with a certain spin projection is occupied multiplied by the corresponding tunneling rate. It is also assumed that a relatively high voltage U is applied between the electrodes, so the trap is located at such an energy E that the corresponding state in the normal electrode is always occupied, while the state in the ferromagnet is empty. A generalization to lower voltages and finite temperatures is straightforwardly accomplished by weighting the tunneling rates Γ_N and Γ_σ with the Fermi distribution $f(E)$ and $(1 - f(E + U))$, respectively.

In order to interpret the third term in the right-hand side of (1) we express the density matrix ρ in terms of the spin projections s_x, s_y, and s_z, on the coordinate axis OX, OY, and OZ, correspondingly, in the form

$$\rho = \frac{1}{2}(nI + s_x\sigma_x + s_y\sigma_y + s_z\sigma_z) \tag{7}$$

where I is the unity matrix and σ_i, $i = x, y, z$ are the Pauli matrices. The difference of the Eq. (1) for $\sigma = \pm$ can be written as

$$\frac{d}{dt}s_z = -\Gamma_F s_z - p\Gamma_F n - \omega_L\sin(\Theta)s_y. \tag{8}$$

For completeness we also provide the equation for the site occupation probability n following from summing up the Eq. (1).

$$\frac{d}{dt}n = \Gamma_N(1-n) - \Gamma_F n - p\Gamma_F s_z \tag{9}$$

In the case $p = 0$ one obtains the standard balance equation for the occupation decoupled from the spin. The non-zero spin polarization of the drain electrode involves the spin degree of freedom into the equation for the site occupation, thus affecting the current which results in the resistance dependence on the magnetic field.

Similarly, the sum and difference of Eq. (2) produce the following two equations:

$$\frac{d}{dt}s_x = \omega_L\cos(\Theta)s_y - \Gamma_F s_x \tag{10}$$

$$\frac{d}{dt}s_y = -\omega_L\cos(\Theta)s_x + \omega_L\sin(\Theta)s_z - \Gamma_F s_y \tag{11}$$

The last terms in Eqs. (10) and (11) describe the escape probabilities of the spin being in the XY plane into the ferromagnet. Because the XY plane is perpendicular to the magnetization orientation in the ferromagnet along the OZ axis, the escape probability is the sum of the two probabilities $\frac{\Gamma_+}{2}$ and $\frac{\Gamma_-}{2}$ to tunnel into the states with the spin up and spin down in the ferromagnet, respectively. Their sum

$$\Gamma_F = \frac{\Gamma_+ + \Gamma_-}{2} \tag{12}$$

results, according to (3), in the total rate Γ_F. The Eqs. (9)–(11) are conveniently written in the vector form

$$\frac{d}{dt}\mathbf{s} = -\Gamma_F\mathbf{s} - \mathbf{p}\Gamma_F n + [\mathbf{s}\times\boldsymbol{\omega}_L], \tag{13}$$

where $\mathbf{s} = (s_x, s_y, s_z)$ and $\mathbf{p} = (0, 0, p)$.

Eq. (13) describes the dynamics of the spin in the presence of a

magnetic field on the trap coupled to the leads, where one of which is ferromagnetic. Without the terms proportional to Γ_F the equation resembles the Bloch equation for spin dynamics, however, without relaxation and dephasing. Spin relaxation and dephasing can become quite important, especially at elevated temperatures, where experiments on spin injection into a semiconductor by pushing the electrical current through a ferromagnet-oxide-semiconductor structure are performed. Similar to the Bloch Eq. [20], one can generalize (13) by including the spin lifetime T_1 and the dephasing time T_2 [16]:

$$\frac{d}{dt}\mathbf{s} = -\Gamma_F\mathbf{s} - \mathbf{p}\Gamma_F n + [\mathbf{s}\times\omega_L] - \left(\frac{1}{T_1}-\frac{1}{T_2}\right)\frac{(\mathbf{s}\bullet\omega_L)}{\omega_L}\frac{\omega_L}{\omega_L} + \frac{1}{T_1}s_0\frac{\omega_L}{\omega_L} - \frac{1}{T_2}\mathbf{s} \tag{14}$$

Thereby it is guaranteed that the spin component along the magnetic field **B** relaxes with time T_1 to an equilibrium value s_0, while the perpendicular component dephases with time T_2. At room temperatures $T_2 \cong T_1$.

3. Equilibrium current

The stationary current I due to tunneling via a trap is computed as

$$I = e\Gamma_N(1-n). \tag{15}$$

Solving Eqs. (9) and (14) for the stationary case results in the following expression for the current:

$$I = e\frac{\Gamma_F(\Theta)\Gamma_N}{\Gamma_F(\Theta)+\Gamma_N} \tag{16a}$$

$$\Gamma_F(\Theta) = \Gamma_F\left(1 - p^2\Gamma_F T_1\left\{\frac{\cos^2\Theta}{\Gamma_F T_1+1} + \frac{T_2}{T_1}\frac{\sin^2\Theta(\Gamma_F T_2+1)}{\omega_L^2 T_2^2 + (\Gamma_F T_2+1)^2}\right\}\right) \tag{16b}$$

For comparison with the previously known results we assume that the equilibrium spin at the trap $\mathbf{s}_0 = 0$.

The current (16) differs from the current value, when both electrodes are normal nonmagnetic metals.

$$I = e\frac{\Gamma_F\Gamma_N}{\Gamma_F+\Gamma_N} \tag{17}$$

In particular, the current depends on the angle Θ between the spin quantization axis (magnetic field) and the magnetization orientation.

In the case $T_1 = T_2 \to \infty$, when relaxation and dephasing are ignored, one obtains

$$\Gamma_F(\Theta) = \Gamma_F\left(1 - p^2\left\{\cos^2\Theta + \frac{\sin^2\Theta}{\omega_L^2/\Gamma_F^2+1}\right\}\right). \tag{18}$$

With this result the corresponding expression for the current obtained in [6] is reproduced.

Complementary to the results given in [6], (16) includes the effects of spin relaxation. When $\Gamma_F T_1 = \Gamma_F T_2 \ll 1$, the resistance dependence on the magnetic field is a Lorentzian function with the half-width determined by the inverse spin lifetime. A short spin relaxation time suppresses the spin blockade [6], which appears at small Θ in a similar fashion as the reduction of spin current polarization p (Fig. 2). The strong dephasing (short T_2) suppresses the last term in (16b), which increases the amplitude of the current $I(\Theta)$ (Fig. 2), in contrast to the intuitive expectation that strong decoherence should reduce the effect. Increasing dephasing (decreasing T_2) results in an unusual non-monotonic dependence of the magnetoresistance as a function of the magnetic field **B** perpendicular to the magnetization, with the linewidth decreasing, at shorter T_2 as shown in Fig. 3.

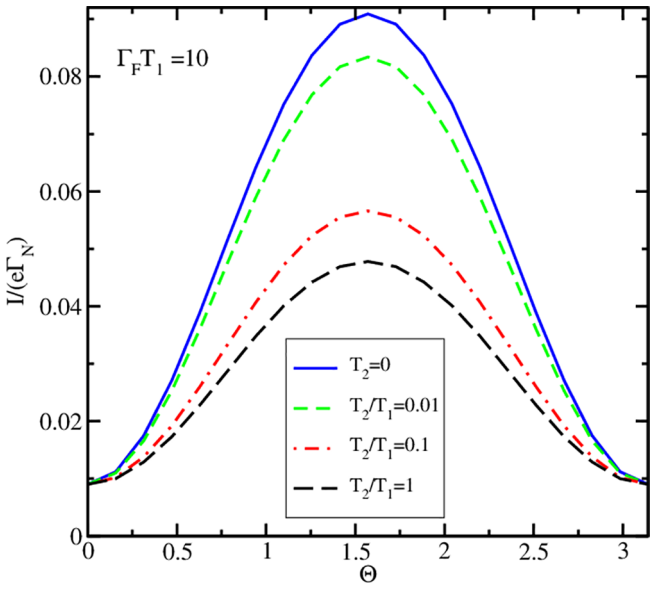

Fig. 2. Current as a function of Θ, for $p = 1$, $\Gamma_N/\Gamma_F = 10$, $\omega_L/\Gamma_F = 1$, $\Gamma_F T_1 = 10$, and several values of T_2/T_1.

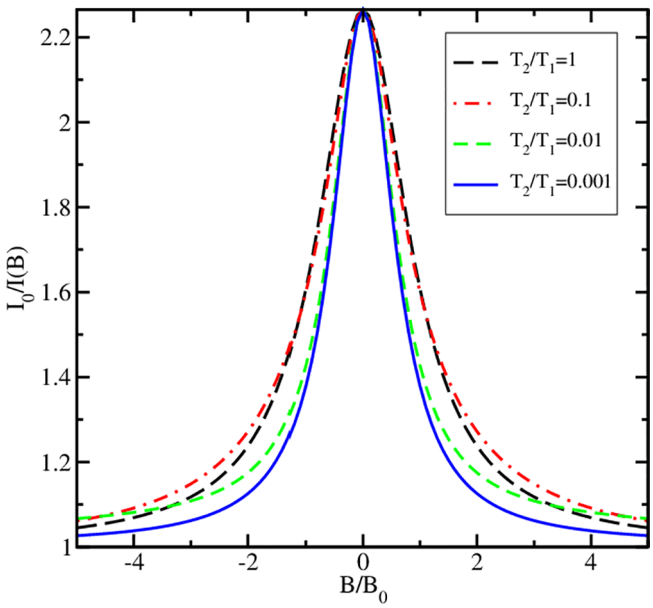

Fig. 3. Magnetoresistance signal as a function of the perpendicular magnetic field **B** for several T_2/T_1, for $p = 0.8$ and $\Gamma_F T_1 = 10$. The field $\mathbf{B}_0$ is perpendicular to the magnetization in the ferromagnet.

4. Charge transfer process and shot noise

4.1. Spin-independent hopping

In the case of spin-independent hopping the master equation for the trap occupation obtained from (9) for $\mathbf{s} = 0$ is

$$\frac{d}{dt}n = \Gamma_N(1-n) - \Gamma_F n. \tag{19}$$

The charge transfer process described by (19) is represented by cyclic repetition of the two consecutive electron hops, namely first from the normal source electrode on the trap with the rate Γ_N followed by the electron escape from the trap to the normal drain electrode with the rate Γ_F [18,21]. The current is then evaluated by averaging over a large number N of cycles the charge transferred, devided by the total time.

Each hopping event is independent and happens at random times τ_1 and τ_2, respectively. The probability p for an electron to perform a hope at time $\tau_{1(2)}$ is equal to

$$p_{N(F)}(\tau_{1(2)}) = \Gamma_{N(F)} \exp(-\Gamma_{N(F)}\tau_{1(2)}). \tag{20}$$

It can then be immediately shown that the stationary current I is equal to

$$I = \frac{Ne}{\sum_{i=1}^{N}(\tau_1+\tau_2)_i} = \frac{e}{<\tau_1>+<\tau_2>}. \tag{21}$$

(21) coincides with (17) because the averaged times $<\tau_{1(2)}> = \sum_{i=1}^{N}(\tau_{1(2)})_i/N$ evaluated with (21) are equal to

$$<\tau_{1(2)}> = \int_0^\infty \tau_{1(2)} p_{N(F)}(\tau_{1(2)}) d\tau_{1(2)} = \frac{1}{\Gamma_{N(F)}}. \tag{22}$$

In order to investigate the current fluctuations at low frequency ω we need to evaluate the current-current correlator (23).

$$S(\omega) = 2\int_{-\infty}^{\infty} (I(t+x)I(t) - I^2)\cos\omega x dx \tag{23}$$

I the stationary current (21). For a series of the consecutive electron hops the correlator (23) can be evaluated by using the following expression [22]:

$$S(\omega=0) = 2eI\left(\frac{N\sum_{i=1}^{N}(\tau_1+\tau_2)_i^2}{\left(\sum_{i=1}^{N}(\tau_1+\tau_2)_i\right)^2} - 1\right) \tag{24}$$

In the case of spin-independent hopping (24) can be evaluated with the help of (22) to get for the Fano factor F:

$$F = \frac{S(\omega=0)}{2eI} = \left(\frac{\langle(\tau_1+\tau_2)\rangle^2}{\langle\tau_1+\tau_2^2\rangle} - 1\right) = \frac{\Gamma_N^2+\Gamma_F^2}{(\Gamma_N+\Gamma_F)^2} \tag{25}$$

The Fano factor determines the discretness of the charge transfer. Indeed, when $\Gamma_N \ll \Gamma_F$, the transport is determined by the "bottleneck" junction with the smallest rate. In this case the Fano factor equals one, indicating that the electrons are transferred through the bottleneck junction consecutively one by one.

In the general case of trap-assisted hopping within the model (19) the Fano factor (25) is less than one.

4.2. Spin-dependent hopping

In the case of spin-dependent hopping the hopping process again consists of two consecutive hops from the normal source electrode to the trap and an escape from the trap to the ferromagnetic electrode. While the first process is characterised by a single rate Γ_N, the escape is characterised by a matrix because of the coupling between the the spin and the occupation at the trap as described by the master Eqs. (9) and (14), and it is not immeditely clear how to determine the escape rates.

The escape probability $P(t)$ from the trap in the case of spin-independent hopping is described as

$$P(t) = 1 - n(t), \tag{26}$$

where $n(t)$ is the solution of the differential equation

$$\frac{d}{dt}n(t) = -\Gamma_F n(t) \tag{27}$$

with the initial condition $n(t=0)=1$.

In the case of a ferromagnetic drain electrode the escape rate is still determined by (26), while the trap occupation$n(t)$ is determined from [23]:

$$\frac{d}{dt}\begin{pmatrix} n \\ s_x \\ s_y \\ s_z \end{pmatrix} = -\mathbf{A}\begin{pmatrix} n \\ s_x \\ s_y \\ s_z \end{pmatrix} \tag{28a}$$

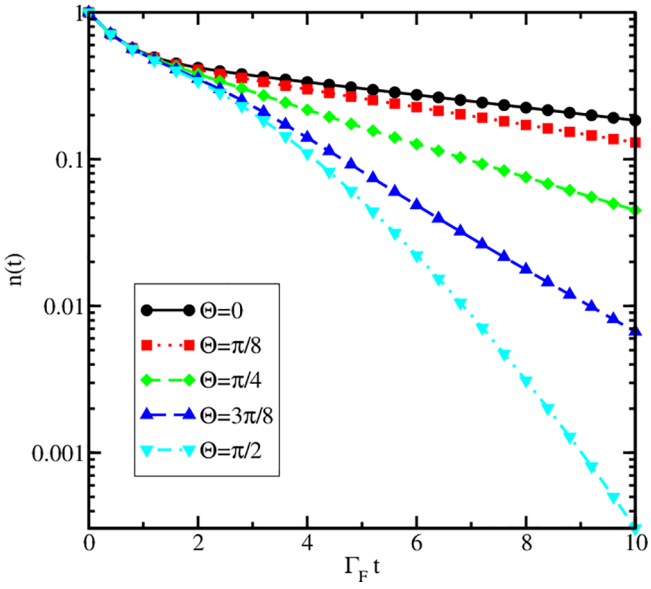

Fig. 4. Probability distribution of escape times for $\Gamma_F = \omega_L$ and $|\mathbf{p}| = 0.9$.

The 4 × 4 relaxation matrix **A** is written in the coordinate system with the OZ axis parallel to the magnetic field **B:**

$$\mathbf{A} = \begin{pmatrix} \Gamma_F & p\Gamma_F\sin(\Theta) & 0 & p\Gamma_F\cos(\Theta) \\ p\Gamma_F\sin(\Theta) & \Gamma_F + \frac{1}{T_2} & \omega_L & 0 \\ 0 & -\omega_L & \Gamma_F + \frac{1}{T_2} & 0 \\ p\Gamma_F\cos(\Theta) & 0 & 0 & \Gamma_F + \frac{1}{T_1} \end{pmatrix} \tag{28b}$$

Because the trap is populated by hopping from the normal electrode, spin-up and spin-down states are occupied with equal probabilities. Thus, the initial spin at the trap is zero, and the initial condition for (28a) is

$$\begin{pmatrix} n \\ s_x \\ s_y \\ s_z \end{pmatrix}(t=0) = \begin{pmatrix} 1 \\ 0 \\ 0 \\ 0 \end{pmatrix}. \tag{29}$$

Fig. 4 shows the typical behavior of $n(t)$ obtained from (28a), (28b) and (29). In contrast to spin-independent tunneling, the probability is not determined by a single exponential but a more complex behavior.

We evaluate the current and the shot noise by a Monte Carlo technique. The charge transport consists of a series of repeated cycles. An electron jumps from the normal electrode to the trap with the rate Γ_N, and then escapes from the trap to the ferromagnetic electrode with the probability $P(t)$ (26). Double occupancy of the trap is prohibited by the Coulomb repulsion. One electron charge is transferred at each cycle during the time $\tau_1 + \tau_2$. The random time τ_1 is evaluated by a direct Monte Carlo technique according to the escape probability $P_1(t) = 1 - \exp(-t/\Gamma_N)$. The time τ_2 is distributed according to $P_2(t) = 1 - n(t)$ and is evaluated numerically for a known $n(t)$. The total current I is computed from (21) for a large number of cycles N.

Current simulation results are shown in Fig. 5. They are in good agreement with the results from [6]. The current values from [15] are too large for all the directions of the magnetic field except the one, when **B** is parallel to **p**. This implies that the escape rates used in [15] are faster. The escape time distribution probability in [15] is determined by the two tunneling rates from each of the Zeeman levels renormalized by coupling to the ferromagnetic contact (Fig. 5, dashed lines). This approximation is appropriate only in the case, when the magnetic field is aligned with the magnetization. In the general case the consideration based on the matrix Eq. (28b) is necessary to reproduce

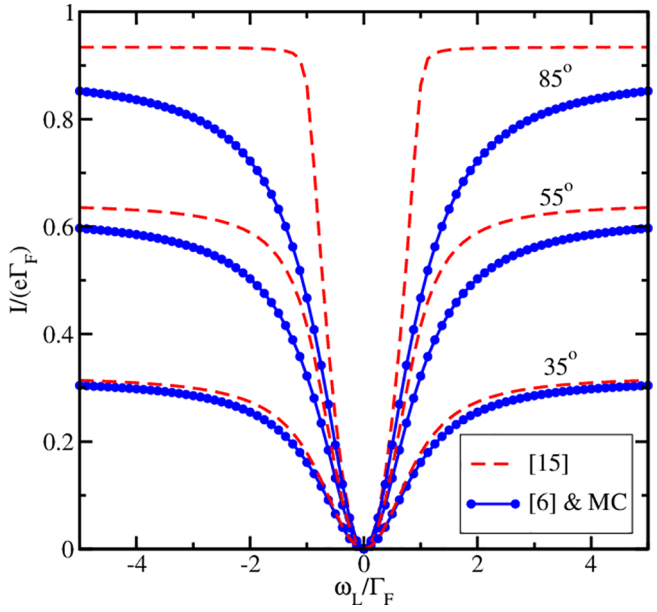

Fig. 5. Comparison of Monte Carlo results (symbols) with the results from [6] and [15]. $|\mathbf{p}| = 1$, $\Gamma_N = 8\Gamma_F$.

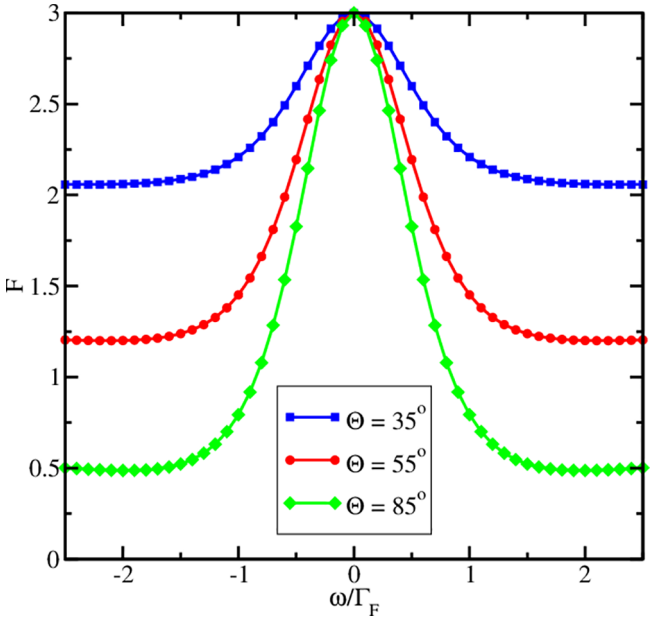

Fig. 6. Fano factor at spin-dependent hopping as a function of the Larmor frequency, for several angles between the magnetization and the magnetic field.

the correct transition probabilities and currents. The reason is that the time evolution (28) is defined by four eigenvalues $\gamma_{\pm}^{+}$ and $\gamma_{\pm}^{-}$ of the 4×4 relaxation matrix $\mathbf{A}$ (28b).

$$\gamma_{\pm}^{+} = \Gamma_F \pm \left(\frac{1}{2}(p^2\Gamma_F^2 - \omega_L^2) + \sqrt{\frac{(p^2\Gamma_F^2 - \omega_L^2)^2}{4} + \omega_L^2 p^2 \Gamma_F^2 \cos^2\Theta} \right)^{1/2} \tag{30a}$$

$$\gamma_{\pm}^{-} = \Gamma_F \pm \left(\frac{1}{2}(p^2\Gamma_F^2 - \omega_L^2) - \sqrt{\frac{(p^2\Gamma_F^2 - \omega_L^2)^2}{4} + \omega_L^2 p^2 \Gamma_F^2 \cos^2\Theta} \right)^{1/2} \tag{30b}$$

But only the two values $\gamma_{\pm}^{+}$ out of the four were considered in [15]. This explains [23] the controversy between the results [6,15] in Fig. 5.

4.3. Shot noise at spin-dependent hopping

We now evaluate the shot noise and the Fano factor (25) for the case of spin-dependent hopping in the normal/ferromagnetic metal structure. The results shown in Fig. 6 indicate that, in contrast to the spin-independent hopping, the shot noise is significantly enhanced, especially at small magnetic fields. Indeed, the value of the Fano factor is larger than one for arbitrary Θ and magnetic fields, for which $\omega_L < \Gamma_F$, and for arbitrary magnetic fields, if $\Theta < 55°$. The maximal value of the Fano factor is three. It implies that the electrons are transferred in bunches of three electrons in average separated by longer waiting times. This is due to the presence of the two electron conducting channels with the spin parallel/antiparallel to the magnetization with high/low conductivities. The transmitted electron is allowed to use only one channel.

The maximal value of the shot noise is observed, when the magnetic field is small or parallel to the magnetization of the drain electrode. In this case the transport is fully determined by the two relaxation rates $\gamma_{\pm}^{+}$, because $\gamma_{-}^{+} \ll \gamma_{+}^{+}$, $\langle t_N + t_F \rangle^2 \approx \frac{1}{4\gamma_{-}^{+2}}$, and $\langle (t_N + t_F) \rangle^2 \approx \frac{1}{\gamma_{-}^{+2}}$, which leads to the Fano factor

$$F = \left(\frac{\langle (t_N + t_F) \rangle^2}{\langle t_N + t_F^2 \rangle} - 1 \right) \approx 3 \tag{31}$$

which is consistent with the maximum value observed in Fig. 6. Measuring the shot noise at tunneling experiments between the normal and ferromagnetic electrodes is essential as the enhanced shot noise provides an additional evidence for spin-dependent tunneling in these structures.

5. Spin-dependent transport between ferromagnetic contacts

We consider the spin-dependent hopping transport between two non-colinear ferromagnetic contacts (Fig. 7) with the interface current polarizations $\mathbf{p}_{S,D} = \frac{\Gamma_{S,D}^{+} - \Gamma_{S,D}^{-}}{2\Gamma_{S,D}} \frac{\mathbf{M}_{S,D}}{M_{S,D}}$ in the source (drain) electrode with the saturation magnetization $M_{S(D)}$, and $\Gamma_{S,D} = \frac{\Gamma_{S,D}^{+} + \Gamma_{S,D}^{-}}{2}$ In order to determine the escape probability $P_2(t) = 1 - n(t)$ from the trap one has to solve Eqs. (28a) and (28b), however, with a modified initial condition for the spin as the ferromagnetic source electrode injects electrons with the spin defined by the source polarization vector, namely:

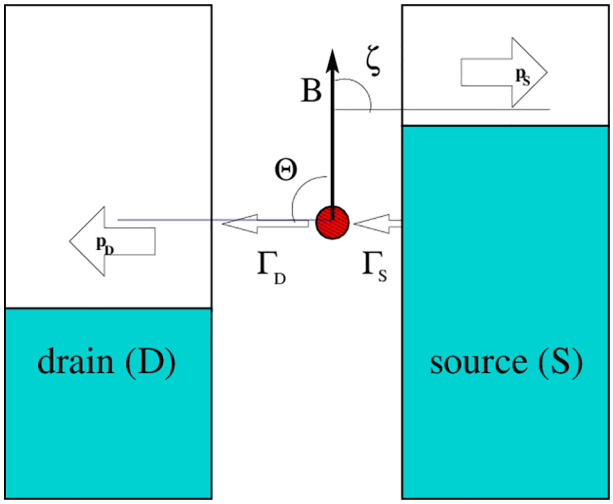

Fig. 7. Trap-assited tunneling between the source and drain ferromagnetic electrodes. The magnetizations along the polarizations $\mathbf{p}_{S,D}$ are non-colinear and form angles Θ, ζ with respect to the magnetic field $\mathbf{B}$. (For simplicity $\mathbf{p}_{S,D}$ and $\mathbf{B}$ are lying within the same plane: $\varphi = 0$).

$$\begin{pmatrix} n \\ s_x \\ s_y \\ s_z \end{pmatrix}(t=0) = \begin{pmatrix} 1 \\ p_S \sin\zeta\cos\varphi \\ p_S \sin\zeta\sin\varphi \\ p_S \cos\zeta \end{pmatrix} \tag{32}$$

The tunneling rate from the source ferromagnet to the trap does not depend on its polarization and is just the sum of the tunneling rates with the spin-up and the spin-down projections on the axis oriented along the source polarization $\mathbf{p}_S$.

$$\Gamma_{S\to Trap} = \Gamma_S^+ + \Gamma_S^- = 2\Gamma_S \tag{33}$$

Now, when the spin-dependent tunneling rates are determined, the calculation of the current and the shot noise is straightforward by using a Monte Carlo technique [24]. Before doing this, we evaluate the expression for the tunneling current analytically in the next section.

5.1. Stationary current

In order to evaluate the stationary current in the case of spin-dependent hopping between ferromagnetic electrodes one has to solve the master equation for the trap occupation and spin [24].

$$\frac{d}{dt}\begin{pmatrix} n \\ s_x \\ s_y \\ s_z \end{pmatrix} = 2\Gamma_S(1-n)\begin{pmatrix} 1 \\ p_S \sin\zeta\cos\varphi \\ p_S \sin\zeta\sin\varphi \\ p_S \cos\zeta \end{pmatrix} - \mathbf{A}\begin{pmatrix} n \\ s_x \\ s_y \\ s_z \end{pmatrix} \tag{34}$$

The phenomenological spin relaxation time T_1 and the spin dephasing time T_2 are introduced to take these processes into account on the dynamics of the spin projections on the axes in the coordinate system $\mathbf{s}=(s_x, s_y, s_z)$ with the OZ axis parallel to the magnetic field $\mathbf{B}$. Θ is the angle between the magnetic field and the drain magnetization, and the angles (ζ, φ) define the orientation of the source magnetization relative to the magnetic field $\mathbf{B}$ (Fig. 7).

The current I through a trap due to the spin-dependent trap-assisted hopping can be alternatively found from the stationary solution from (34) for the average trap occupation n following [23]

$$I = 2e\Gamma_S(1-n), \tag{35a}$$

$$I = e\frac{2\Gamma_F(\Theta)\Gamma_S}{\Gamma_F(\Theta)+\Gamma_2(\Theta,\zeta,\varphi)}, \tag{35b}$$

$$\Gamma_F(\Theta) = \Gamma_D\left(1 - p_D^2\Gamma_D T_1\left\{\frac{\cos^2\Theta}{\Gamma_D T_1+1} + \frac{T_2}{T_1}\frac{\sin^2\Theta(\Gamma_D T_2+1)}{\omega_L^2 T_2^2 + (\Gamma_D T_2+1)^2}\right\}\right), \tag{35c}$$

$$\Gamma_2(\Theta,\zeta,\varphi) = 2\Gamma_S\left(1 - p_S p_D \Gamma_D T_1\left\{\frac{\cos\Theta\cos\zeta}{\Gamma_D T_1+1} + \frac{T_2}{T_1}\frac{\sin\Theta\sin\zeta(\Gamma_F T_2+1)}{\omega_L^2 T_2^2 + (\Gamma_D T_2+1)^2}\left(\cos\varphi - \frac{\omega_L T_2}{\Gamma_D T_2+1}\sin\varphi\right)\right\}\right). \tag{35d}$$

Fig. 8 shows the dependence of current as a function of Θ for several values of ζ, for $\varphi = 0$ (both magnetizatons are in the same plane with $\mathbf{B}$, Fig. 7), $\Gamma_S = 5\Gamma_D$, $\omega_L = \Gamma_D/2$, $p_S = p_D = 0.8$, without spin relaxation. The current has a maximum at $\Theta = \zeta$, when the contact magnetizations are parallel. In addition, there is a smaller current increase at $\Theta = -\zeta$. The second maximum value is found to increase with the magnetic field, when the spin precession is faster. Because the spin precesses within the cone passing through both magnetizations, the rise of the magnetic field and the frequency of precession increases the chance of an electron to escape.

A high magnetic field suppresses the terms with *sine* functions (35). The terms can also be suppressed by dephasing ($T_2 = 0$). Fig. 9 shows the effect of spin dephasing and relaxation on the charge current due to trap-assisted tunneling through an MTJ, for $\zeta = 0$. The difference between the maximum and the minimum currents is enhanced at strong

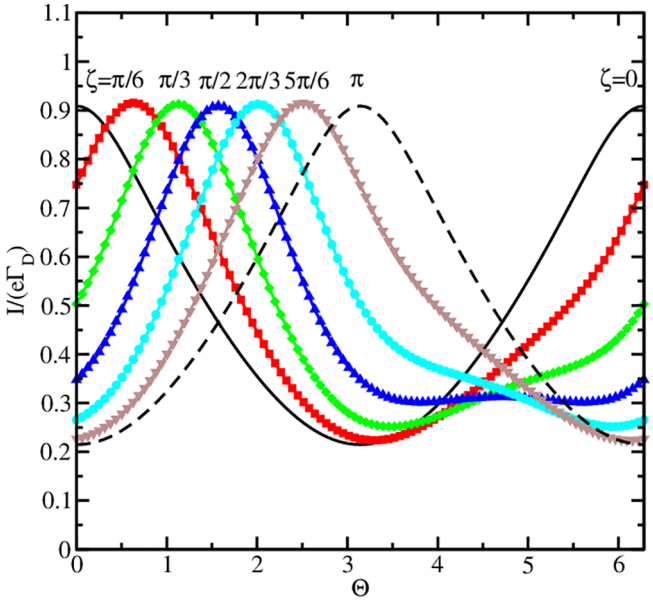

Fig. 8. Trap-assited tunneling current between the source and drain ferromagnetic electrode as a function of Θ for several ζ. The parameters are: $\Gamma_S = 5\Gamma_D$, $\omega_L = \Gamma_D/2$, $p_S = p_D = 0.8$. It is assumed that there is no spin relaxation nor dephasing.

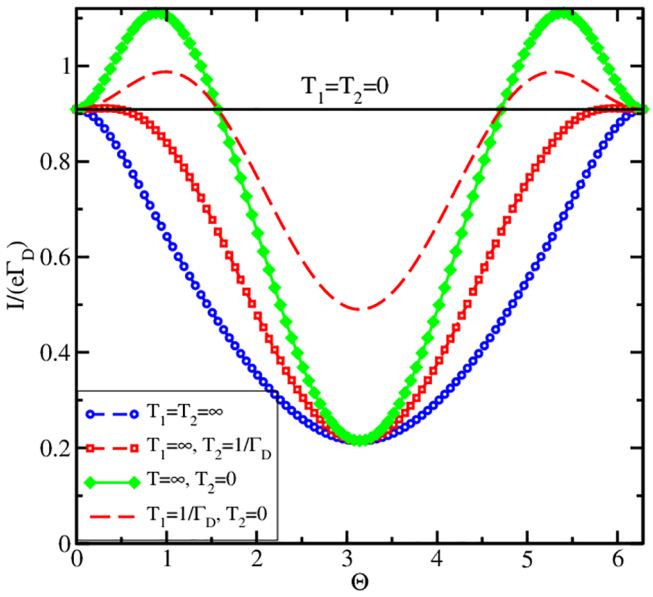

Fig. 9. Trap-assited tunneling current between the source and drain ferromagnetic electrode as a function of Θ for $\zeta = 0$. The parameters are: $\Gamma_S = 5\Gamma_D$, $\omega_L = \Gamma_D/2$, $p_S = p_D = 0.8$. It is assumed that there is no spin relaxation.

dephasing. One peculiarity is that the maximal current is achieved when $\Theta \neq \zeta$ as shown in Fig. 9. Importantly, the TMR at spin-dependent hopping with strong dephasing is larger than the TMR at direct tunneling [23], indicating the potential of spin-dependent hopping for MTJs' transport properties optimization.

5.2. Shot noise

We have checked that the results for current calculations obtained by simulating the charge transfer as a series of consecutive electron hops based on (28), (32) and performing the time averaging by means of the Monte Carlo technique reproduce the stationary current values (34) in Figs. 8 and 9.

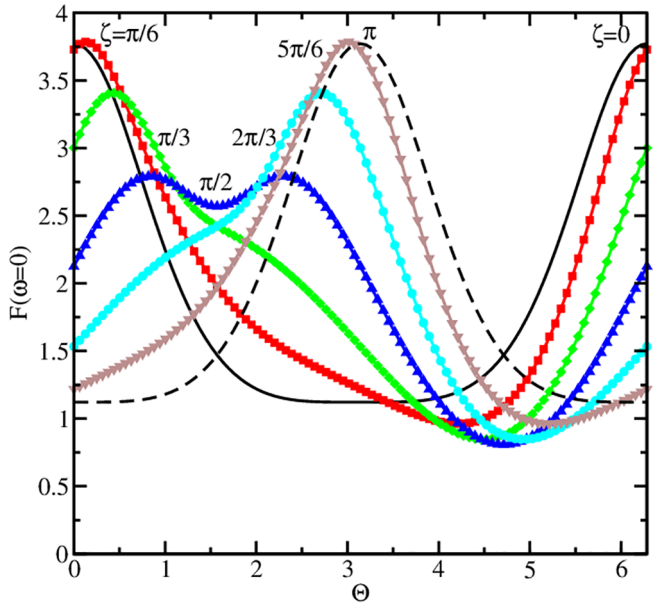

Fig. 10. Shot noise at trap-assisted tunneling between the source and drain ferromagnetic electrode as a function of Θ for severalζ. The parameters are: $\Gamma_S = 5\Gamma_D$, $\omega_L = \Gamma_D/2$, $p_S = p_D = 0.8$. It is assumed that there is no spin relaxation.

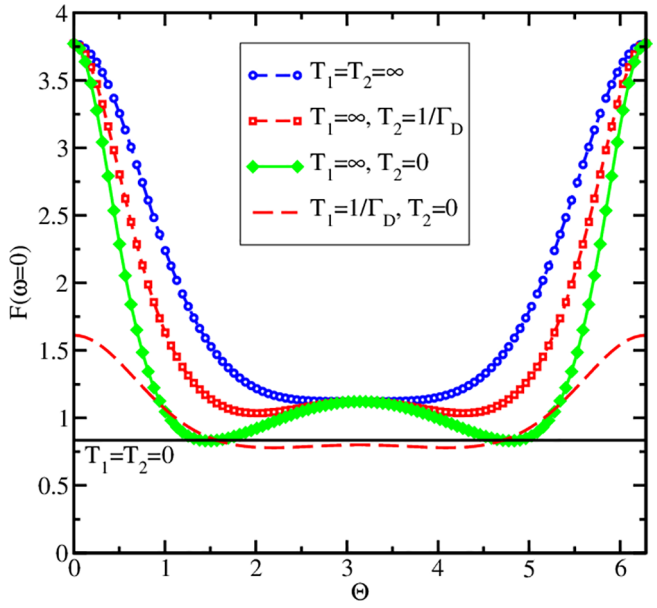

Fig. 11. Effect of spin relaxation and dephasing on shot noise at spin-dependent trap-assisted hopping between the source and drain ferromagnetic electrode as a function of Θ for $\zeta = 0$. The parameters are: $\Gamma_S = 5\Gamma_D$, $\omega_L = \Gamma_D/2$, $p_S = p_D = 0.8$.

We proceed to evaluating the shot noise by means of (28), (32), and (25). Fig. 10 shows the shot noise normalized by the current evaluated with (8) as a function of Θ for several values of ζ, $\Gamma_N = 10\Gamma_F$, $\omega_L = \Gamma_F/2$, $p = p_2 = 0.8$. The Fano factor F shown in Fig. 10 is significantly enhanced around $\Theta \approx \zeta \approx 0$. It correlates with the large current values shown in Fig. 8 for the same parameters. We note that this behavior is opposite to the one predicted for spin-dependent trap-assisted hopping between the normal and ferromagnetic electrodes, where the noise has a maximum (Fig. 6) at the minimum of the current (Fig. 5). Although the correlations between the current and the noise are opposite in MTJs and at transport between the normal metal and ferromagnet, in both cases the noise enhancement and the Fano factor above one are due to spin correlations.

In the following we interpret the enhancement of the shot noise in the structures with two ferromagnetic contacts. For the drain magnetization parallel to the magnetic field (Θ=0) the transport is determined by the two channels with the rates $\Gamma_D(1 \pm p_D)$. The probability to excite the channels is proportional to the injection rates $\Gamma_S(1 \pm p_S)$ for $\zeta \approx 0$. The time-dependent charge transfer process is governed by the bursts of high currents through the fast channel, separated by long periods with low current through the slow channel. As the probability to excite the fast channel is largest at ζ=0, the current is maximal. At the same time, the charge transferred during the current bursts between the two periods of low currents is maximal, which determines the high value of the shot noise in the high current state of MTJs.

Fig. 11 displays the influence of spin dephasing and relaxation on the low frequency noise for ζ=0. Spin relaxation suppresses spin correlations and brings the noise to the level of spin-independent hopping (10), which is below one. As follows from Fig. 9, strong spin dephasing increases the differences between the minimum and the maximum values. At the same time the current maximum is shifted to finite Θ. By inspecting Fig. 11 we conclude that the shot noise is significantly decreased at the current maximum as the Fano factor is significantly suppressed compared to its highest value at $\Theta = 0$ for finite Θ. In conclusion, strong spin dephasing at spin-dependent hopping enhances the TMR, while it simultaneously reduces the noise level.

6. Conclusion

The master equation describing the dynamics of the electron occupation and the spin on a trap in oxide sandwiched between a ferromagnetic and a normal or ferromagnetic metal contact is augmented by including the spin relaxation and dephasing. The electron current and the shot noise at trap-assisted hopping in magnetic tunnel junctions are evaluated. It is demonstrated that the spin-induced correlations play a critical role in determining the current modulation and especially the noise level.

It is proven that only in the case when the magnetic field is parallel to the drain magnetization the spin-dependent tunneling rates are determined by the two spin-up and spin-down eigenvalues of a 4 × 4 non-symmetric transition matrix. In the general case all four eigenvalues contribute to the transition rates. This resolves the controversy in the literature and explains the discrepancy between the approaches [6] and [15], where only two eigenstates were considered.

Without spin relaxation and dephasing the shot noise and the Fano factor at spin-dependent hopping are significantly enhanced above their value at spin-independent hopping due to the Pauli spin blockade, if the magnetic field is parallel to the magnetization of the ferromagnetic contacts.

Strong spin relaxation reduces the magnetoresistance modulation. However, the role of dephasing on the magnetoresistance and the noise is not always detrimental. An unusual non-monotonic dependence of the magnetoresistance as a function of dephasing is predicted. Surprisingly, spin dephasing enhances the TMR and simultaneously reduces the noise level rendering the potential of spin-dependent hopping for practical applications.

Acknowledgment

The financial support by the Austrian Federal Ministry for Digital and Economic Affairs and the National Foundation for Research, Technology and Development is gratefully acknowledged.

References

[1] Apalkov D, Dieny B, Slaughter JM. Magnetoresistive random access memory. Proc IEEE 2016;104:1796–830.
[2] Averin DV, Likharev KK. Coulomb blockade of single-electron tunneling, and coherent oscillations in small tunnel junctions. J Low Temp Phys 1986;62:345–73.
[3] Ono NK, Austing DG, Tokura Y, Tarucha S. Current rectification by pauli exclusion

in a weakly coupled double quantum dot system. Science 2002;297:1313.
[4] Wang Y, Sahin-Tiras K, Harmon NJ, Wohlgenannt M, Flatté ME. Immense magnetic response of exciplex light emission due to correlated spin-charge dynamics. Phys Rev X 2016;6.
[5] Brataas A, Bauer GEW, Kelly PJ. Non-collinear magnetoelectronics. Phys Rep 2006;427:157–255.
[6] Song Y, Dery H. Magnetic-field-modulated resonant tunneling in ferromagnetic-insulator-nonmagnetic junctions. Phys Rev Lett 2014;113:047205.
[7] Dash SP, Sharma S, Patel RS, de Jong MP, Jansen R. Electrical creation of spin polarization in silicon at room temperature. Nature 2009;462:491–1484.
[8] Li CH, van't Erve OMJ, Jonker BT. Electrical injection and detection of spin accumulation in silicon at 500 K with magnetic metal/silicon dioxide contacts. Nature Commun 2011;2:245.
[9] Jansen R. Silicon spintronics. Nat Mater 2012;11:400–8.
[10] Sverdlov V, Selberherr S. Silicon spintronics: advances and challenges. Phys Rep 2015;585:1–40.
[11] Spiesser A, Saito H, Jansen R, Yuasa Sh, Ando K. Large spin accumulation voltages in epitaxial Mn_5Ge_3 contacts on Ge without an oxide tunnel barrier. Phys Rev B 2014;90. Art. 205213.
[12] Jeon K-R, Saito H, Yuasa Sh, Jansen R. Energy dispersion of tunnel spin polarization extracted from thermal and electrical spin currents. Phys Rev B 2015;91:155305.
[13] Spiesser A, Saito H, Fujita Y, et al. Giant spin accumulation in silicon nonlocal spin-transport devices. Phys Rev Appl 2017;8.
[14] Tahara T, Ando Y, Kameno M, et al. Observation of large spin accumulation voltages in nondegenerate si spin devices due to spin drift effect: experiments and theory. Phys Rev B 2016;93.
[15] Yue Z, Prestgard MC, Tiwari A, Raikh ME. Resonant magnetotunneling between normal and ferromagnetic electrodes in relation to the three-terminal spin transport. Phys Rev B 2015;91:195316.
[16] Sverdlov V, Selberherr S. Spin-dependent trap-assisted tunneling including spin relaxation at room temperature 10-13 August 2015, Basel, Switzerland Program and Abstract Book of the 8th International School and Conference on Spintronics and Quantum Information Technology (SPINTECH)2015. p. 114.
[17] Sverdlov V, Weinbub J, Selberherr S. Spin-dependent trap-assisted tunneling in magnetic tunnel junctions: a monte carlo study. Abstract Book International Workshop on Computational Nanotechnology. 2017. p. 88–90.
[18] Bakhvalov S, Kazacha GS, Likharev KK, Serdyukova SI. Single-electron Solitons in one-dimensional tunnel structures. Sov Phys JETP 1989;68:581.
[19] Sverdlov V, Korotkov AN, Likharev KK. Shot-Noise suppression at two-dimensional hopping. Phys Rev B 2001;63:081302(R).
[20] Bloch F. Nuclear induction. Phys Rev 1946;70:460.
[21] Korotkov AN. Intrinsic Noise of the Single-electron Transistor. Phys Rev B 1994;49:10381.
[22] Kinkhabwala J, Korotkov AN. Shot noise at hopping via two sites. Phys Rev B 2000;62:R7727–30.
[23] Sverdlov V, Weinbub J, Selberherr S. Current in magnetic tunnel junctions at spin-dependent hopping ISBN: 978-3-901578-31-1 Abstracts of the Workshop on Innovative Devices and Systems (WINDS)2017. p. 87–8.
[24] Sverdlov V, Selberherr S. Current and shot noise at spin-dependent hopping in magnetic tunnel junctions. Book of Abstracts EUROSOI-ULIS. 2018. p. 107–8.